J Appl Electrochem (2009) 39:859–866
DOI 10.1007/s10800-008-9732-y

ORIGINAL PAPER

Influence of hot-pressing temperature on physical and electrochemical performance of catalyst coated membranes for direct methanol fuel cells

Peng Liu · Ge-Ping Yin · Er-Dong Wang · Jian Zhang · Zhen-Bo Wang

Received: 21 March 2008 / Accepted: 18 November 2008 / Published online: 4 December 2008

Abstract The physical and electrochemical performance of a direct methanol fuel cell (DMFC) are improved by optimizing the hot-pressing temperature for fabricating the catalyst coated membrane (CCM) through the decal transfer method. SEM and XRD tests show that the morphology of the catalyst layer and the growth of Pt particles can be greatly influenced by the hot-pressing temperature. The CCM hot-pressed at 185 °C displays the best output performance due to the increase in electrochemical surface area (ESA), and the improved contact between the catalyst layer and the membrane. Although high hot-pressing temperature favors decreased methanol crossover, the performance of the CCM is subject to serious Pt agglomeration and slow mass transport.

Keywords Direct methanol fuel cell · Catalyst coated membrane · Decal transfer method · Hot-pressing temperature · Electrochemical surface area

Abbreviations

DMFC	Direct methanol fuel cell
MEA	Membrane electrode assembly
CCM	Catalyst coated membrane
CDM	Catalyzed diffusion medium
ESA	Electrochemical surface area
EIS	Electrochemical impedance spectroscopy
OCV	Open circuit voltage
DC	Direct current
CV	Cyclic voltammetry
SEM	Scanning electron microscope
XRD	X-ray diffraction
ORR	Oxygen reduction reaction
MOR	Methanol oxidation reaction
DHE	Dynamic hydrogen electrode
LSV	Linear sweep voltammetry

P. Liu · G.-P. Yin (✉) · E.-D. Wang · J. Zhang · Z.-B. Wang
School of Chemical Engineering and Technology,
Harbin Institute of Technology, Harbin 150006,
People's Republic of China
e-mail: yingphit@hit.edu.cn

1 Introduction

The direct methanol fuel cell (DMFC) has attracted increasing attention as a potential portable power source due to high energy density, simple system and dense fuel storage [1–3]. However, some technical issues, such as poor electro-catalytic activities of Pt or Pt alloy catalysts [4–6], and serious methanol permeation through the electrolyte [7–9] restrict its practical application of DMFC.

As the key component of DMFC, membrane electrode assembly (MEA) plays an important role in the cell performance. Conventional MEA is fabricated by hot-pressing the catalyzed diffusion medium (CDM) electrodes on to each side of a polymer electrolyte membrane. Even at a high catalyst loading, the CDM is subject to low Pt utilization due to insufficient contact sites between the electrolyte and the electrode [10]. In recent years much effort has been devoted to improving the performance of the MEA by achieving more effective electrolyte-catalyst-reactant 'triple-phase boundaries' (TPB) [11–14]. Catalyst coated membranes (CCM), with the electrocatalyst applied to the surface of the electrolyte directly so as to enhance the TPB and obtain a better Pt utilization, offer new opportunities to produce low catalyst loading MEAs. In comparison with CDM, CCM exhibited significantly higher electrochemical surface area and lower electrode polarization resistance for the methanol oxidation reaction at the same electrocatalyst loading [15].

Mao et al. [16] and Lindermeir et al. [17] discovered that the configuration of CCMs improved DMFC performance.

The decal transfer method is a popular technique to fabricate the CCM by transferring the catalyst layer from the Teflon support onto the electrolyte membrane during hot-pressing [18]. The preparation process is critical to the performance of the CCM [19, 20]. As reported by Zhang et al. [21] and Liang et al. [22], hot-pressing conditions greatly influenced the performance of the CDM. However, little research has focussed on the optimal hot-pressing conditions for decal CCM. In this study, physical and electrochemical techniques were used to investigate the effect of hot-pressing temperature on the electrochemical surface area, anode and cathode polarization, as well as methanol crossover behavior.

2 Experimental

2.1 Fabrication of CCMs

Nafion® 117 membranes were pretreated in a water bath at 80 °C, following the sequence in 3 wt% H_2O_2 solution, ultra-pure water, 0.5 mol L^{-1} NaOH solution, and ultra-pure water [23].

Cathode and anode diffusion layers were used as the mass transport mediums for CCMs. The cathode gas diffusion layer was a 25 wt% wet-proof carbon paper (TGP-H-090, Toray Industries, Inc.) scraped with a suspension of Vulcan XC-72 carbon black (E-TEK Co., Ltd.) and PTFE at a ratio of 3:1. The anode diffusion layer was an untreated carbon paper coated with a microporous layer consisting of 95 wt% carbon black and 5 wt% Nafion® ionomer. The loading of carbon black on both the cathode diffusion layer and anode diffusion layer was 1.5 mg cm^{-2}.

Commercial 30 wt% Pt–Ru (1:1)/C (HiSPEC 5000, Johnson Matthey Plc.) and homemade 40 wt% Pt/C, based on the impregnation–reduction method [24, 25], were used as anode and cathode catalysts, respectively. The catalyst ink, which was a mixture of catalyst, 5 wt% Nafion® solution (1,100 equivalent weight), 0.5 mol L^{-1} NaOH solution and isopropyl alcohol, was prepared by continuously stirring in an ultrasonic bath for at least 20 min. The weight ratio of metal, Nafion® ionomer and NaOH was 3:1:1 for both anode and cathode. Then, the catalyst inks were sprayed on the Teflon sheets to prepare four pairs of anode and cathode. For each electrode, the geometric active area was 5 cm^2 and the Pt loading was 2.0 mg cm^{-2}. After drying in a vacuum oven at 80 °C for 30 min, the catalyst layers were transferred onto the membranes from Teflon supports by hot-pressing at 165, 175, 185, and 195 °C, respectively, under a pressure of 15 MPa for 90 s. Subsequently, the newly formed CCMs (denoted as CCM-1, CCM-2, CCM-3, and CCM-4, respectively) were re-protonated in 0.5 mol L^{-1} H_2SO_4 at 80 °C for 1 h. Finally, the CCMs were combined with the diffusion layers by hot-pressing under a specific load of 8 MPa at 135 °C for 120 s to form the MEAs.

2.2 Single cell test

The output performance of the CCMs was evaluated with a commercial single cell (ElectroChem Corp.), using a Fuel Cell Testing System (Arbin Instruments Corp.) at 30 °C. A 2 mol L^{-1} aqueous methanol solution was pumped to the anode side at a flow rate of 2 mL min^{-1}, and pure oxygen was supplied to the cathode side at a flow rate of 50 mL min^{-1} under ambient pressure. The cell voltage was varied from open circuit voltage (OCV) to 0.15 V.

2.3 Physical analysis

Surface morphology and interfacial microstructure of the CCMs were observed by a Sirion 200 Scanning Electron Microscope (FEI Electron Optics, Netherlands). XRD analysis was conducted on the original catalysts and the samples scraped from the CCMs to characterize the change in the Pt particles after the hot-pressing procedure. The XRD patterns were recorded by a Japan D/max-rB X-ray diffractometer, using a Cu Kα radiation source at a tube current of 100 mA and a tube voltage of 40 kV, with a scan rate of 5° min^{-1}.

2.4 Electrochemical measurements

All the electrochemical measurements were carried out at 30 °C. The cathodes of the CCMs are denoted as CCM-1C, CCM-2C, CCM-3C, and CCM-4C, and the anodes as CCM-1A, CCM-2A, CCM-3A, and CCM-4A, respectively.

The electrochemical impedance spectroscopy (EIS) of the CCMs was tested by a CHI 604B Electrochemical Analyzer (Shanghai Chen-Hua Instruments Corp.) when the cells were operated at a current density of 15 mA cm^{-2}. Furthermore, the EIS of the anodes was tested at the same current density, with the cathodes as dynamic hydrogen electrodes (DHE) by feeding humidified H_2 at a flow rate of 50 mL min^{-1}. The AC amplitude was set at 0.005 V and the frequency ranged from 10^5 to 10^{-2} Hz. The diagrams were analyzed with a fitting software, ZSimpWin.

Cyclic voltammetry (CV) was employed to determine the electrochemical surface area (ESA) of the cathodes. During the test, the cathode was protected by pure Ar at a flow rate of 200 mL min^{-1}. The CV sweep was performed at a scan rate of 0.01 V s^{-1} between 0.05 and 1.2 V versus the anode, which was designed as the DHE. The ESA of the cathode was obtained according to Eq. 1 [26], where [Pt] represents the platinum loading (mg cm^{-2}) on the electrode, Q_H denotes the charge (mC cm^{-2}) for hydrogen

desorption [25], and 0.21 is the charge (mC cm^{-2}) required to oxidize a monolayer of H_2 on bright Pt.

$$\mathrm{ESA} = \frac{Q_{\mathrm{H}}}{[\mathrm{Pt}] \times 0.21} \quad (1)$$

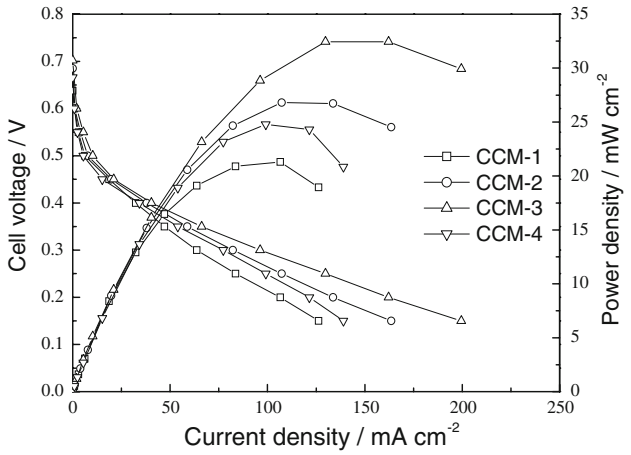

Fig. 1 $I \sim V$ and power density curves of CCMs hot-pressed at different temperatures. $T_{cell} = T_{fuel} = T_{O2} = 30°C$. Anode: 2 mol L^{-1} methanol solution, a flow rate of 2 mL min^{-1}, Pt–Ru loading: 3 mg cm^{-2}. Cathode: O_2 at atmospheric pressure, a flow rate of 200 mL min^{-1}, Pt loading: 2 mg cm^{-2}

Steady-state polarization curves of ORR and MOR were investigated by an HA-151 Potentiostat/Galvanostat Apparatus (Hokuto Denko Inc. Japan). When the steady-state curve of ORR was measured at the cathode, the anode served as a DHE, and vice versa.

The methanol crossover rate was estimated by the limiting current density at the cathode. During the test, a 2 mol L^{-1} methanol solution was fed to the anode at 2 mL min^{-1}. Simultaneously, linear sweep voltammetry (LSV) was executed at the cathode at 0.01 V s^{-1}, with a delivery of pure Ar at 200 mL min^{-1}. The anode, where only the reduction of H^+ to H_2 took place, can be regarded as a DHE [27, 28].

3 Results and discussion

3.1 Single cell performance

The $I \sim V$ and power density curves of the CCMs at 30 °C are shown in Fig. 1. CCM-3 hot-pressed at 185 °C displays the best output performance, with a peak power density of 32 mW cm^{-2}. The better performance at higher hot-pressing temperature can be attributed to the improvement in the contact between catalyst layer and the membrane,

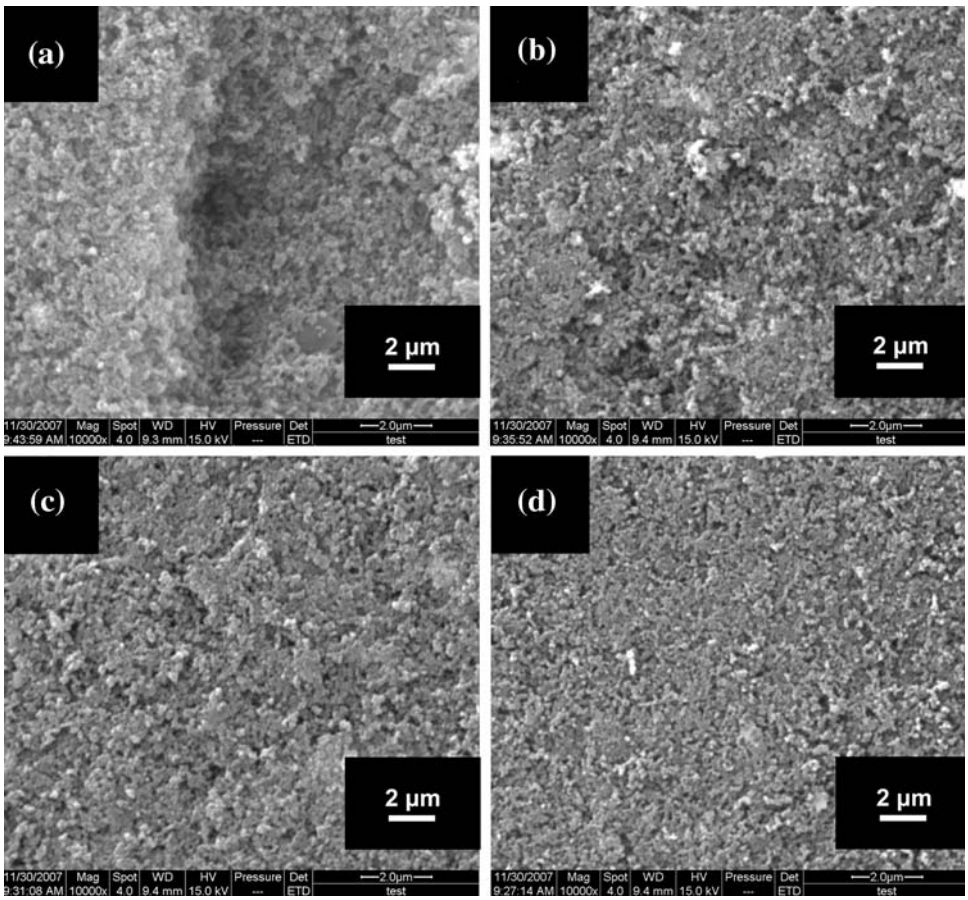

Fig. 2 Surface micrographs of the catalyst layers hot-pressed at different temperatures. **a** 165 °C, **b** 175 °C, **c** 185 °C, **d** 195 °C

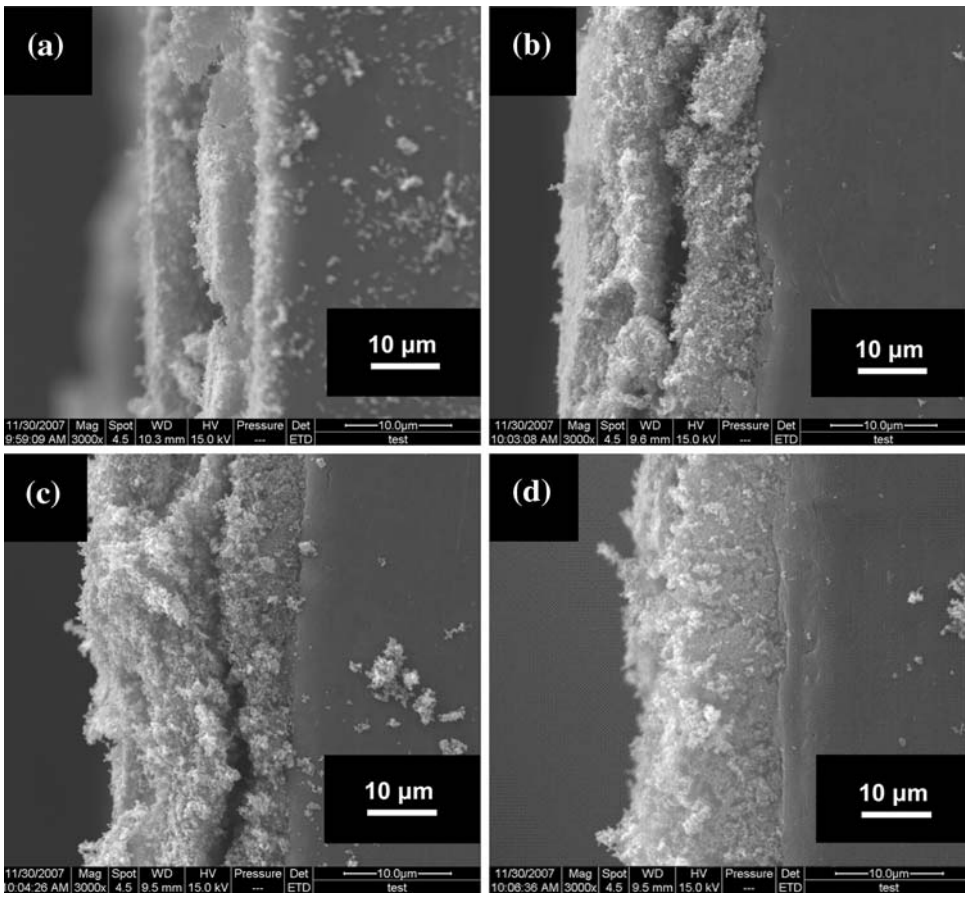

Fig. 3 Cross-sectional micrographs of the CCMs hot-pressed at different temperatures. **a** 165 °C, **b** 175 °C, **c** 185 °C, **d** 195 °C

which will be further verified in the SEM test. However, the output performance of CCM-4 hot-pressed at 195 °C is inferior to those of CCM-3 and CCM-2.

3.2 Morphological characteristics

Figure 2 shows the effect of hot-pressing temperature on the surface morphology of the catalyst layer. For the CCMs hot-pressed at 165–175 °C, the loose surface microstructure with delamination and gaps suggests a weak combination of the catalyst layer components. When the hot-pressing temperature increases to 185 °C, the catalyst layer with homogeneous microporous frameworks is obtained, and thus even distribution of electrochemical active sites and smooth mass transports can be expected. However, when the CCM is hot-pressed at an even higher temperature (195 °C), the catalyst layer becomes so dense that the mass transport passages were significantly decreased. Figure 3 presents the cross-section images of the CCMs hot-pressed at different tempertures. The contact between the catalyst layer and the membrane gradually improved with increase in hot-pressing temperature.

XRD patterns of the original Pt/C and Pt–Ru/C, as well as the samples scraped from the catalyst layers, are shown in Fig. 4. The typical peak of the (111) plane of a Pt crystallite at 40° is used to calculate the average size of Pt particles based on Scherrer's formula [29]. The particle sizes of the cathode and anode catalysts are listed in Table 1. For the cathode catalysts, a size increase from 2.7 to 6.0 nm indicates obvious growth of Pt partcles at high temperature. By contrast, the growth of anode catalyst particles is much smaller after the hot-pressing step. As reported previously [18, 22], the oxides of Ru, forming during the preparation procedure of the CCM, could serve as a dispersing agent and prevent agglomeration of Pt particles.

3.3 Electrochemical activities of the electrodes

Nyquist diagrams (depicted by dots) of the total cells and the anodes are illustrated in Fig. 5a and b, respectively. It is noteworthy that the DC polarization was controlled at a low current density of 15 mA cm^{-2}, where mass transport limitation was not expected. For each plot in Fig. 5a, the first and second semi-circles are attributed to the oxygen reduction reaction (ORR) and methanol oxidation reaction (MOR), respectively [30], and the loop in the low frequency region is caused by the slow relaxation of the adsorbed CO [31]. However, the spectra are not sensitive

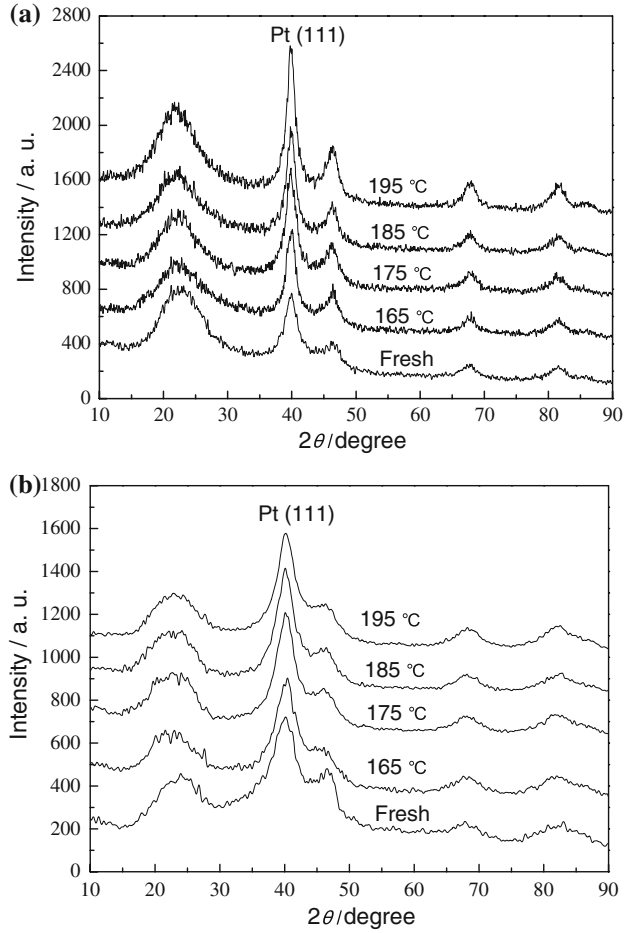

Fig. 4 XRD patterns of original catalyst and samples scraped from catalyst layers. **a** Pt/C; **b** Pt–Ru/C

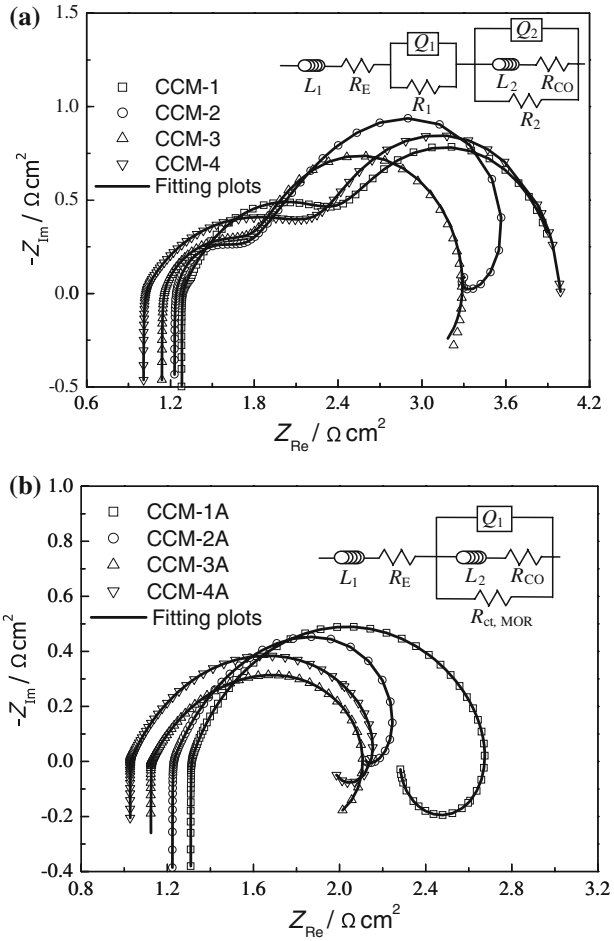

Fig. 5 Nyquist diagrams (dots) of CCMs at a direct current density of 15 mA cm^{-2}, and fitting diagrams (lines) based on possible equivalent circuits. **a** Total cell; **b** Anode

enough to separate the cathode process and the anode process due to oxidation of the methanol at the cathode. A possible equivalent circuit in Fig. 5a is used to describe the cell system, and the fitting parameters of the CCMs are summarized in Table 2. The internal resistance of the cell, symbolized as R_E, becomes lower with increase in hot-pressing temperature,.which mainly results from the decreased interfacial resistance between the catalyst layer and the membrane. The reaction resistance of the total cell ($R_{r,CELL}$) decreases from 2.42 to 1.56 Ω cm^2, and then increases to 2.23 Ω cm^2 when the hot-pressing temperature rises from 165 to 195 °C. The change in $R_{r,CELL}$ confirms the results of the single cell test. However, the cathode and anode reaction resistances cannot be distinguished from the cell reaction resistance [32]; thus it is necessary to analyze the EIS of the anodes. The equivalent circuit in Fig. 5b is suggested to model the anode process and the fitting results are listed in Table 3. The anode reaction resistances ($R_{r,A}$) vary from 0.57 to 0.97 Ω cm^2, as determined through the charge transfer resistances of the elementary reactions, $R_{ct,MOR}$ and R_{CO}. Accordingly, it can be deduced that the cathode reaction resistances are 1.45, 1.05, 0.99, and 1.37 Ω cm^2, corresponding to the cathodes hot-pressed at 165, 175, 185, and 195 °C, respectively.

Cyclic voltammograms of Pt/C at the cathodes are shown in Fig. 6, which reveals the relationship between the cathode ESA and the hot-pressing temperature. The ESAs

Table 1 Average particle sizes of the fresh catalysts and those after hot-pressing procedure

Catalysts	Cathode					Anode				
	Fresh	165 °C	175 °C	185 °C	195 °C	Fresh	165 °C	175 °C	185 °C	195 °C
Average particle size/nm	2.7	3.7	4.2	4.9	6.0	2.6	3.1	3.3	3.4	3.7

Table 2 Fitting results of the resistance elements for the cells

Resistances/Ω cm^2	CCM-1	CCM-2	CCM-3	CCM-4
R_E	1.30	1.21	1.09	0.99
R_1	1.27	0.88	0.79	1.21
R_2	1.60	1.47	1.26	1.43
R_{CO}	4.12	2.95	2.01	3.61
$R_{r,CELL} = R_1 + (R_2 \times R_{CO})/(R_2 + R_{CO})$	2.42	1.86	1.56	2.23

Table 3 Fitting results of the resistance elements for the anodes

Resistances/Ω cm^2	CCM-1A	CCM-2A	CCM-3A	CCM-4A
R_E	1.31	1.20	1.12	1.01
$R_{ct,MOR}$	1.46	1.37	1.16	1.30
R_{CO}	2.92	1.96	1.13	2.56
$R_{r,A} = R_{ct,MOR} \times R_{CO}/(R_{ct,MOR} + R_{CO})$	0.97	0.81	0.57	0.86

of the cathodes are determined by integrating the areas of the hydrogen desorption peaks. As shown in Fig. 6, CCM-3C hot-pressed at 185 °C exhibits the highest ESA of 362.2 cm^2 mg_{Pt}^{-1}. In other words, the Pt utilization in the electrochemical reaction is most sufficient at this hot-pressing temperature. For CCM-4C, significant agglomeration of nano-sized Pt particles at 195 °C leads to the loss of the ESA. It is demonstrated that the poor performance of CCM-4 is related to the degradation of electro-catalytic activity of the cathode.

The steady-state polarization curves at the cathodes and the anodes are presented in Fig. 7a and b, respectively. The equilibrium potentials for ORR and MOR are approximately 1.0 V and 0.2 V versus DHE, respectively. The steady-state curves are determined by the interaction of electrochemical, ohmic, and concentration polarization. In the low current density regions, as presented in Fig. 7, both ORR and MOR rates are governed by the electrochemical activity of the electrodes. With increase in current density, the curves gradually deviate from each other due to the different ohmic losses between working electrodes and

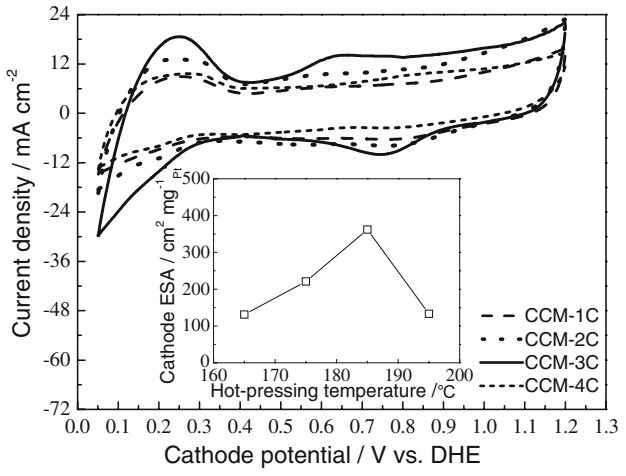

Fig. 6 Cyclic voltammograms of Pt at CCM cathodes, at a scan rate of 0.01 V s^{-1}, in a potential range between 0.05 V and 1.2 V versus DHE

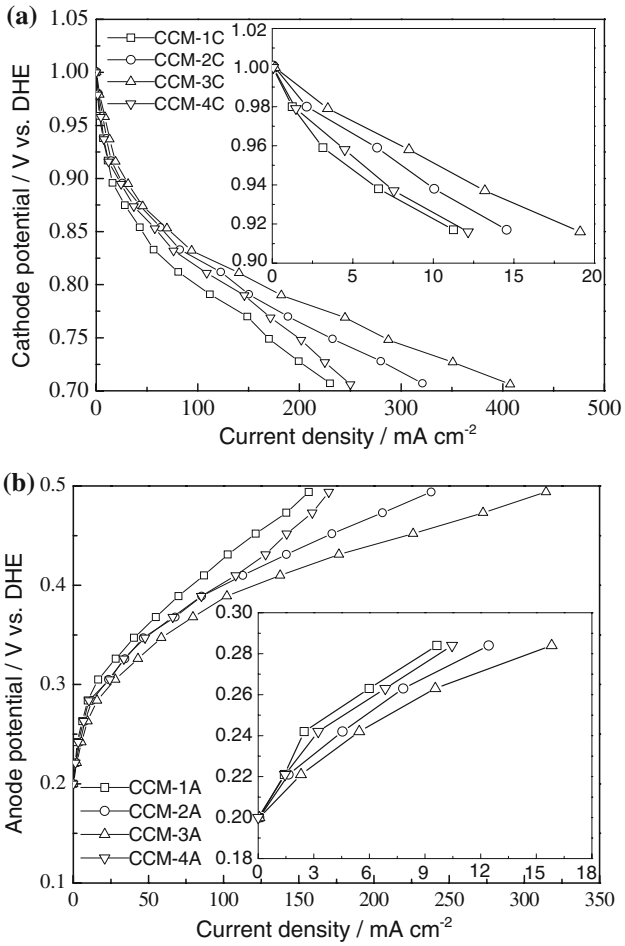

Fig. 7 Steady-state polarization curves of ORR and MOR versus DHE. **a** Cathodes, **b** Anodes

counter electrodes (reference electrodes), including the ionic resistance of the electrolyte, the electronic resistances of the electrodes, and interfacial resistances especially. In the high current density regions, the electrode processes are dominated by slow mass transport. CCM-4, with a dense catalyst layer, suffers from serious concentration polarization at both anode and cathode.

3.4 Effect of hot-pressing temperature on methanol permeation

Methanol crossover was explored by controlling MOR at the high cathode potential region, where the reaction is governed by the permeation rate of the methanol. As shown in Fig. 8, the peak current density of methanol crossover decreases with rise in hot-pressing temperature. CCM-4 yields the lowest limiting permeation current density of 8 mA cm^{-2}, which results from slow methanol transport from the anode to the cathode. As is well known, the anode with high electro-catalytic activity promotes oxidation of the methanol on the anode side. Moreover, the catalyst layer hot-pressed at 195 °C displays a dense morphology according to SEM results. Despite the low electrocatalytic activity, the catalyst layer hot-pressed at high temperature can act as a dense barrier to greatly reduce the methanol crossover through the membrane.

4 Conclusions

Physical and electrochemical measurements were carried out to investigate the effect of hot-pressing temperature on the performance of the CCM prepared by the decal transfer method. High hot-pressing temperature is considered to be a positive factor for the reduction in interfacial resistance and the enhancement of triple-phase boundaries. Moreover, the dense catalyst layer forming at high temperature plays an important role in limiting methanol crossover. However, with increase in hot-pressing temperature, the growth of Pt particles and the decrease in porosity are unfavorable for the electro-catalytic activity and the mass transport. The single DMFC with the CCM hot-pressed at 185 °C exhibits the best output performance, resulting from high electrochemical surface area and low internal resistance.

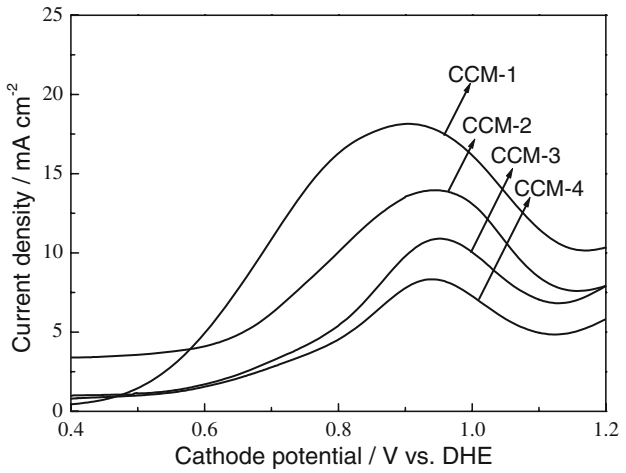

Fig. 8 Linear sweep voltammograms of methanol permeating through the membranes at the cathodes

Acknowledgement The authors are grateful for financial support by Natural Science Foundation of China (No. 20606007 and No. 50872027).

References

1. Kunimatsu M, Okada T (2004) Electrochem Solid State Lett 7:A389
2. Ren XM, Zelenay P, Thomas S et al (2000) J Power Sources 86:111
3. Dillon R, Srinivasan S, Aricò AS et al (2004) J Power Sources 127:112
4. Saha MS, Li RY, Sun XL et al (2007) Electrochem Commun 9:2229
5. Shao YY, Yin GP, Gao YZ (2007) J Power Sources 171:558
6. Su Y, Xue XZ, Xu WL et al (2006) Electrochim Acta 51:4316
7. Han JH, Liu HT (2007) J Power Sources 164:166
8. Jung EH, Jung UH, Yang TH et al (2007) Int J Hydrog Energy 32:903
9. Song JM, Miyatake KJ, Uchida H et al (2006) Electrochim Acta 51:4497
10. Liu FQ, Wang CY (2006) Electrochim Acta 52:1417
11. Reshetenko TV, Kim HT, Lee HK et al (2006) J Power Sources 160:925
12. Wilson MS, Valerio JA, Gottesfeld S (1995) Electrochim Acta 40:355
13. Uchida M, Fukuoka Y, Sugawara Y et al (1998) J Electrochem Soc 145:3708
14. Shao YY, Yin GP, Wang ZB et al (2007) J Power Sources 167:235
15. Tang HL, Wang SL, Pan M et al (2007) Electrochim Acta 52:3714
16. Mao Q, Sun GQ, Wang SL et al (2007) Electrochim Acta 52:6763
17. Lindermeir A, Rosenthal G, Kunz U et al (2004) J Power Sources 129:180
18. Wilson MS, Gottesfeld S (1992) J Appl Electrochem 22:1
19. Song SQ, Liang ZX, Zhou WJ et al (2005) J Power Sources 145:495
20. Wang ZL, Liu Y, Linkov VM et al (2006) J Power Sources 160:326
21. Zhang J, Yin GP, Wang ZB et al (2006) J Power Sources 160:1035
22. Liang ZX, Zhao TS, Xu C et al (2007) Electrochim Acta 53:894
23. Liu P, Yin GP, Du CY (2008) Electrochem Commun 10:1471
24. Wang ZB, Yin GP, Shi PF et al (2006) Electrochem Solid State Lett 9:A13
25. Tian JH, Wang FB, Shan ZQ et al (2004) J Appl Electrochem 34:461
26. Maillard F, Martin M, Gloaguen F et al (2002) Electrochim Acta 47:3431

27. Ren XM, Springer TE, Zawodzinski TA et al (2000) J Electrochem Soc 147:466
28. Mu S, Tang H, Wan Z et al (2005) Electrochem Commun 7:143
29. Radmilovic V, Gasteiger HA, Ross PN (1995) J Catal 154:98
30. Reshetenko TV, Kim HT, Kweon HJ (2008) Electrochim Acta 53:3043
31. Müller JT, Urban PM, Hölderich WF (1999) J Power Sources 84:157
32. Jeon MK, Won JY, Oh KS et al (2007) Electrochim Acta 53:447